Geochemistry of orbicular diorite from the Grenville Front zone, eastern Labrador

J. VICTOR OWEN

Department of Geology, Saint Mary's University, Halifax, N.S. Canada B3H 3C3

Abstract

Orbicules in diorite from the Grenville Front zone of eastern Labrador consist of biotite- and/or hornblende-studded, dioritic cores enclosed by fine-grained shell structures alternately enriched and depleted in biotite. The orbicules occur in a mesocratic, quartz-bearing matrix. Epidote of inferred magmatic origin occurs in all parts of the rock. Plagioclase in the matrix is relatively sodic, and biotite more ferroan than in the orbicules, suggesting that the matrix material has the most evolved composition, and crystallized last.

The diorite is unusually aluminous (orbicules: 24.9–27.4 wt.% Al_2O_3; matrix: 22.4–23.6% Al_2O_3) and calcic (orbicules: 7.0–8.4 wt.% CaO; matrix: 6.0–6.9% CaO); it shows a positive Eu anomaly, and has elevated Sr concentrations (1800–2500 ppm Sr), demonstrating that, compositionally, it resembles a plagioclase cumulate. Mass-balance calculations suggest that the orbicule cores had a crystal/melt ratio of ≤5. This accounts for the extreme fractionation of the rock (e.g., in orbicules, Zr <5 ppm). Compared with fractional crystallization patterns, variation diagrams show counter-trends (e.g. the siliceous matrix contains elevated TiO_2) or scatter for several components, suggesting that the crystal/melt ratio governed some of the geochemical characteristics of the diorite.

The presence of coarse mafic clots containing primary epidote, biotite and/or hornblende testify to an elevated water content in the orbicule cores. The shell magma apparently formed as a result of the interaction of supercooled orbicule core fluids with the matrix magma, and tended to serve as a reservoir for alkalis and Fe. Alkalis and Ca diffused in opposite directions, possibly as a result of a temperature gradient at the orbicule/matrix interface. This, however, requires decoupling of the thermodiffusional behaviour of alkalis and femic components in hydrated intermediate magma, which contrasts with documented Soret diffusion in mafic systems.

The solidification of the shell magma prior to the orbicule cores and matrix is attributed to dewatering, consistent with the fine grain size of the shell structures. Except where remobilized core material has disrupted the shells, the cores crystallized in isolation from the matrix, which fractionated toward a more evolved composition.

KEYWORDS: diorite, orbicule, geochemistry, Grenville Front, Labrador

Introduction

ORBICULAR rocks on Run By Guess Island, eastern Labrador, are unusual insofar as they contain epidote of probable magmatic origin; the shell structures lack comb textures and are not nucleated on exotic xenoliths. On the basis of morphology, mineralogy and mineral chemistry, the orbicule cores were interpreted (Owen, 1991) to have originated as water-rich magma globules on which rhythmic shells crystallized. Bulk geochemical data are used in this paper to evaluate and refine this crystallization model.

Petrography and mineral chemistry

Orbicule cores are relatively leucocratic compared with the matrix. Both are medium- to coarse-grained, and consist of plagioclase, hornblende, biotite, epidote and magnetite ± titanite. In addition, accessory quartz and K-feldspar occur in the matrix. The shell structures are relatively fine grained and lack hornblende. Dark shells are enriched in biotite, epidote and magnetite ± titanite. In places, leucocratic patches a few centimetres in diameter occur within the matrix. These are partly enclosed by incipient shell structures, and are interpreted as embryonic orbicules. They are henceforth referred to as proto-orbicules.

Plagioclase in the orbicules is more calcic (in orbicule cores: An_{45} to An_{51}) than plagioclase in the matrix (An_{35}). The anorthite content of plagioclase progressively decreases (An_{48} to An_{37}) in successive (i.e. outward from the core) shells.

In contrast, biotite does not show systematic variations in different shells (i.e. $X_{Mg} \sim 0.40$). The most magnesian biotite ($X_{Mg} = 0.66$) occurs as inclusions in quartz-free hornblende in orbicule cores, whereas more ferroan biotite ($X_{Mg} = 0.51$) mantles the hornblende. The magnesian biotite inclusions are interpreted to have crystallized prior to the amphibole. The most ferroan biotite ($X_{Mg} = 0.34$) occurs in the matrix.

Amphibole is a magnesio-hornblende with X_{Mg} of about 0.55, and with up to 11 wt.% Al_2O_3.

Epidote has a pistacite content of 21–26, and formed early in the paragenetic history of the diorite, implying elevated P_{H20}.

Geochemistry

Procedure. Orbicules in two large samples were sawn free of the matrix, and separated into core- and shell-components. Owing to its arcuate, thinly-layered nature, the shell material could not be further divided, so the dark and light shells were, by necessity, analysed collectively.

Major and selected trace elements (Rb to V in Table 1) were determined by X-ray fluorescence spectrometry using a Philips PW1400 with a Rh-anode X-ray tube. Major element concentrations were determined using fused pellets; trace elements were analysed using pressed powder pellets. Analytical precision, based on replicate analyses, is better than 5% (relative) for major oxides, and generally between 5 and 10% (relative) for trace elements.

In order to more fully characterize the incompatible-element content of the orbicule cores and matrix, the cores of one well-developed orbicule, one proto-orbicule, and the matrix in one sample were also analysed by INAA for the rare earths and Cs, Hf, Ta, Th, U, Sc and Co.

Results. The geochemical data (Table 1) reveal that the diorite is unusually aluminous (orbicules: 24.9–27.4 wt.% Al_2O_3; matrix: 22.4–23.6% Al_2O_3; A/CNK values range between 1.05 and 1.15) and calcic (orbicules: 7.0–8.4 wt.% CaO; matrix: 6.0–6.9% CaO); it contains high concentrations of Sr (1800–2700 ppm) and low concentrations of high field strength elements (HFSE), some of which (e.g. Zr, Nb, Y) are near or below detection limit in the orbicules.

As anticipated by the aluminous and Sr-enriched composition of the diorite, chondrite-normalized rare earth patterns (Fig. 1) for orbicule cores and the matrix have positive Eu anomalies. The orbicule core with the most pronounced Eu anomaly also has the lowest concentration of rare earths.

Some systematic compositional variations are apparent (Fig. 2). Compared to the orbicules, the matrix is relatively siliceous (consistent with the local presence of free quartz), enriched in Zr (mean of four analyses = 25 ppm), with slightly elevated Rb/Sr and alkali concentrations. Orbicule cores and shells tend to have overlapping compositions; however, the cores are relatively magnesian, with Mg' values [Mg' = Mg/(Mg+ 0.9*Fe),wt.%] between 0.18 and 0.31 (Mg' = 0.08–0.13 in the shells). The cores are also more calcic, and have lower TiO_2 contents and Rb/Sr ratios (mean of 5 analyses = 0.006) than the shells (Rb/Sr = 0.008).

The presence of ferroan biotite, sodic plagioclase, K-feldspar and free quartz, and the enrichment in Si, alkalis, Rb/Sr and HFSE demonstrate that the matrix of the orbicules has a relatively evolved composition compared to the orbicules. Mg' in the matrix (Mg' = 0.22), however, exceeds that in the shells. The decoupling of Mg' from other fractionation indicators suggests that abnormal geochemical processes governed the evolution of the dioritic magma.

Interpretation

The geochemical data indicate that, compositionally, the diorite is essentially a plagioclase cumulate, and that the extreme depletion of incompatible trace elements reflects a relatively small volume of interstitial melt. The primitive composition of the orbicules (e.g. Zr contents below detection limit) suggests a high crystal/melt ratio. Compared with other analysed orbicule cores, the proto-orbicule appears to have been

Table 1.   Major, trace, and rare earth element concentrations in orbicular diorite from Run-By-Guess Island, Labrador.

	Sample 1			Sample 2								
	orb core	orb shells	matrix	orb1 core*	orb2 core	orb2 shells	matrix	orb3 core	orb3 shells	matrix	proto-orb	matrix
SiO$_2$(wt%)	55.02	55.06	59.34	53.85	54.94	54.15	58.17	54.97	55.53	56.72	54.62	56.96
TiO$_2$	0.40	0.18	0.24	0.19	0.11	0.38	0.33	0.09	0.32	0.33	0.22	0.34
Al$_2$O$_3$**	25.21	26.28	22.46	26.15	26.43	25.09	22.95	27.41	24.96	23.53	25.50	23.57
Fe$_2$O$_{3(t)}$	3.63	2.29	2.79	1.90	1.55	4.39	2.92	1.09	3.42	3.25	2.49	3.05
MnO	0.03	0.02	0.04	0.03	0.02	0.03	0.04	0.02	0.03	0.04	0.04	0.04
MgO	0.83	0.20	0.75	0.88	0.41	0.45	0.86	0.31	0.52	1.01	1.15	0.81
CaO	6.98	7.45	5.96	8.43	7.67	7.33	6.33	8.35	7.16	6.85	8.21	6.59
Na$_2$O	5.41	5.63	5.36	4.46	5.25	5.52	5.46	4.83	5.48	5.18	4.52	5.39
K$_2$O	1.08	0.50	1.05	0.84	0.64	0.90	1.06	0.62	0.90	1.19	1.06	1.15
P$_2$O$_5$	0.09	0.08	0.11	0.07	0.06	0.12	0.11	0.05	0.11	0.11	0.09	0.13
L.O.I.	0.10	0.10	0.60	0.60	0.60	0.20	0.60	0.20	0.50	0.50	0.50	0.40
Total	98.78	97.79	98.70	97.40	97.68	98.56	98.83	97.94	98.93	98.71	98.40	98.43
Rb(ppm)	27	<5	14	17	12	20	27	9	20	20	17	31
Sr	2554	2514	1838	2430	2667	2483	2167	2553	2370	2185	2276	2125
Ba	667	211	308	280	271	347	470	232	390	467	272	488
Zr	<5	<5	7	<5	<5	<5	18	<5	<5	22	<5	51
Nb	<5	<5	<5	<5	<5	<5	5	<5	5	5	<5	5
Y	5	<5	9	9	<5	8	16	7	9	15	16	20
Cr	10	7	12	14	10	8	14	8	8	13	25	12
Ni	7	<5	<5	6	<5	<5	<5	<5	7	8	7	8
Cu	6	5	<5	7	17	16	10	5	13	9	7	7
Zn	48	28	43	32	24	45	44	21	46	49	35	53
Ga	24	23	23	23	23	25	23	21	21	24	22	23
V	71	51	48	37	25	115	54	17	85	64	47	69
Pb	13	13	14	13	15	14	15	14	12	12	13	12
La	ns	ns	ns	ns	ns	ns	ns	14.72	ns	ns	18.77	20.43
Ce	ns	ns	ns	ns	ns	ns	ns	28.51	ns	ns	39.40	40.07
Nd	ns	ns	ns	ns	ns	ns	ns	10.30	ns	ns	17.93	15.60
Sm	ns	ns	ns	ns	ns	ns	ns	1.72	ns	ns	3.47	2.59
Eu	ns	ns	ns	ns	ns	ns	ns	1.04	ns	ns	1.30	1.08
Tb	ns	ns	ns	ns	ns	ns	ns	0.18	ns	ns	0.33	0.28
Yb	ns	ns	ns	ns	ns	ns	ns	0.63	ns	ns	1.41	0.93
Lu	ns	ns	ns	ns	ns	ns	ns	ND	ns	ns	0.18	0.12
Cs	ns	ns	ns	ns	ns	ns	ns	0.22	ns	ns	0.23	0.38
Hf	ns	ns	ns	ns	ns	ns	ns	0.43	ns	ns	0.44	1.34
Ta	ns	ns	ns	ns	ns	ns	ns	0.81	ns	ns	0.64	0.83
Th	<10	<10	<10	<10	<10	<10	<10	0.29	<10	<10	0.34	1.29
U	ns	ns	ns	ns	ns	ns	ns	ND	ns	ns	ND	0.61
Sc	ns	ns	ns	ns	ns	ns	ns	2.67	ns	ns	8.95	4.05
Co	ns	ns	ns	ns	ns	ns	ns	38.17	ns	ns	28.80	64.65

Notes: * orbicular core contains hornblende; other orbicule cores contain biotite.
**Alumina data may be minimum values, particularly for samples with low oxide totals.
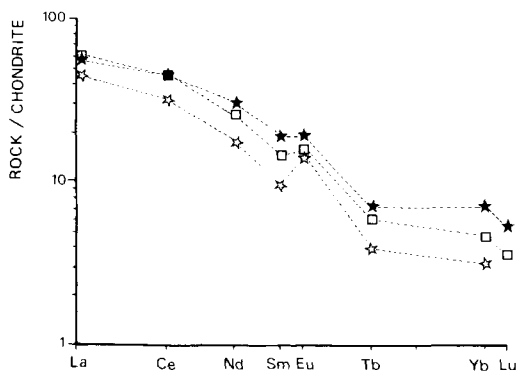ND - not detected; ns - not sought

FIG. 1. Chondrite-normalized REE concentrations in orbicule cores (stars; closed star = proto-orbicule) and the matrix (squares).

relatively melt-rich, as evidenced by higher concentrations of HFSE (e.g. Y, Nb) and rare earths, and lower alumina (Table 1).

A rough estimate of the crystal/melt ratio can be determined by comparing the bulk rock data with the composition of a 'pure' plagioclase cumulate of suitable composition (An$_{45}$). Assuming that the melt fraction had a composition (estimated from mineral compositions and modes) equivalent to orbicule phases other than plagioclase, mass-balance calculations indicate that the proto-orbicule in sample 2 (Table 1) had a crystal/melt ratio of about 5. Because the calculation assumes that plagioclase is exclusively a cumulate phase, this is a maximum value. The absence of typical cumulus/intercumulus textures in the rock precludes estimating the proportion of plagioclase that crystallized from the interstitial liquid.

The enrichment in incompatible elements and depletion in plagioclase components (Ca and Al) suggest that the melt/crystal ratio of the matrix exceeded that of the orbicules.

Origin and geochemical evolution of the orbicules. Unlike many orbicular rocks (see Elliston,
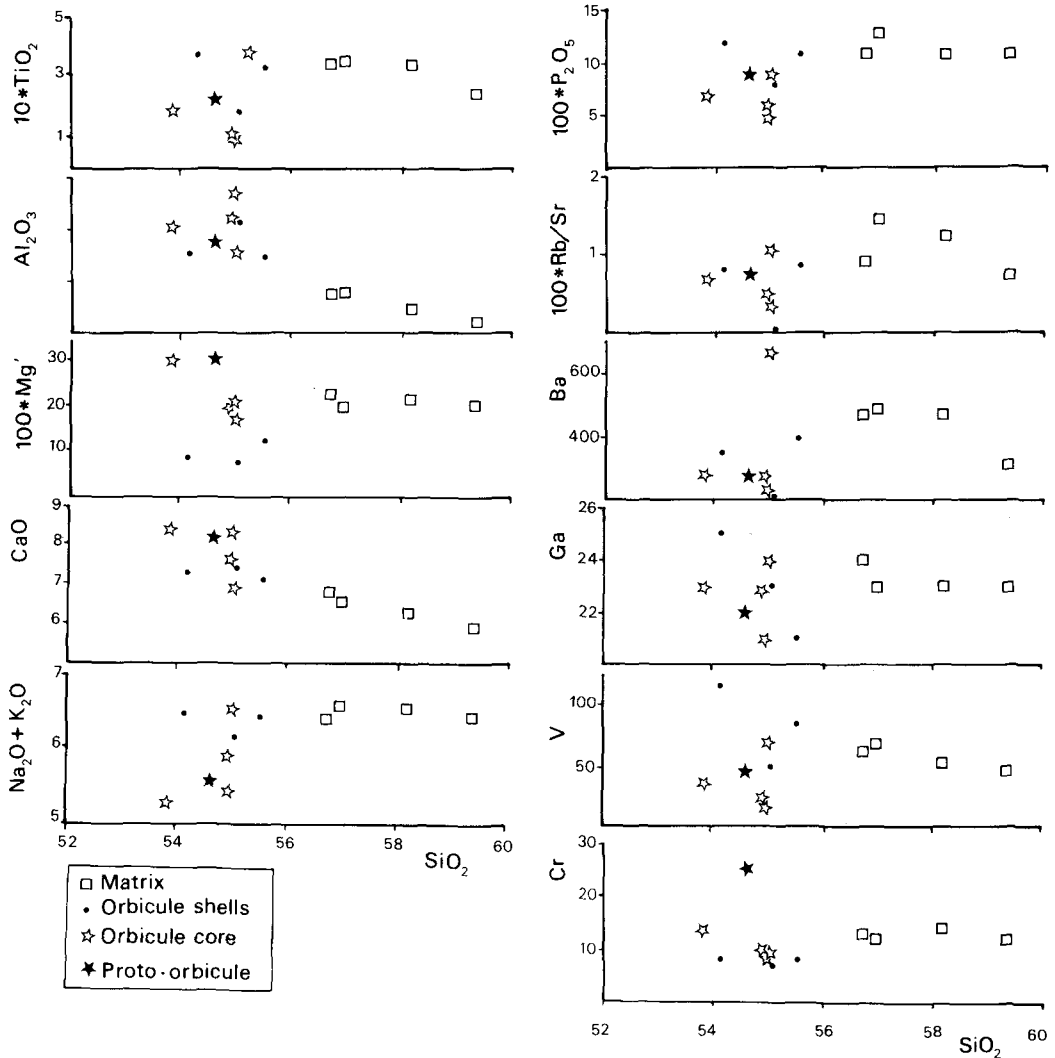
FIG. 2. Compositional variation diagrams showing how selected major cation oxides (in wt.%) and trace elements (in ppm) vary as a function of SiO_2.

1984), shell structures in the orbicular diorite are not nucleated on exotic xenoliths (e.g. of the gneissic country rock), but are cored instead by medium- to coarse-grained diorite. The dioritic orbicule cores are studded with large (to 1.5 cm) biotite and/or hornblende crystals or crystal aggregates. This texture, along with the presence of magmatic epidote, and the disruption of adjacent shells by remobilized core material (Owen, 1991), indicates that the centres of the orbicules contained water-rich melt that remained liquid after the consolidation of the shells. The orbicule cores are commonly in gradational contact with the innermost of the enclosing shell structures. It is therefore unlikely that the orbicule cores represent cognate inclusions (autoliths) of the diorite.

Citing this petrographic evidence, Owen (1991) postulated that the orbicule cores originated as water-rich magma globules upon which the shells nucleated and crystallized (at a temperature below the hornblende liquidus) as supercooled boundary layers. This anticipates (1) the depolymerization of the orbicule magma, enriching this

material in incompatible elements, and (2) the establishment of a temperature gradient at the orbicule/matrix boundary, which would promote temperature-dependent (Soret) diffusion of components, potentially yielding geochemical trends radically different from crystal fractionation patterns. The postulated presence of discrete magma globules does not necessarily imply immiscibility, because discrete volumes of differing magma compositions can coexist without mixing if they have contrasting densities or temperatures (Helz *et al.*, 1989). Indeed, it is unlikely that the orbicules originated as immiscible blebs: they are much larger than immiscible globules (diameter ≤ 50 um) preserved in mafic rocks, and, unlike immiscible liquids (Philpotts, 1982), the compositions of the orbicules and the matrix are not extremely divergent (Table 1).

The depletion, rather than enrichment, of the orbicules in incompatible elements does not negate compelling mineralogic evidence (e.g. liquidus epidote) for elevated P_{H_2O} in the dioritic magma, but is consistent instead with a high crystal/melt ratio. The small amount of melt in the orbicule cores would interfere with crystal fractionation processes, which in any case could have affected the orbicules only in their embryonic stage, prior to consolidation of the enclosing shells. Fractional crystallization cannot, however, be entirely discounted, because variation diagrams (Fig. 2) show that some components (e.g. alkalis) vary smoothly with SiO_2 in a manner compatible with this process.

The possible roles of crystal fractionation and Soret diffusion in the evolution of the dioritic magma are evaluated using a Mg' *versus* Ca/(Ca + Na) [$=X_{Ca}$] plot (Fig. 3). These components vary sympathetically in situations where magma compositions are controlled by fractional crystallization. In contrast, experiments on basalt conducted by Walker and DeLong (1982) show that Mg' and X_{Ca} behave antithetically if Soret diffusion occurred. No comparable experimental data on intermediate magma compositions are available, so the present study assumes that Walker and Delong's (1982) experimental results for mafic systems are pertinent to rocks of dioritic composition.

Fig. 3 shows that there is a positive correlation (R = 0.87) between Mg' and X_{Ca} for the orbicule core data, implying that orbicules with primitive compositions (e.g. proto-orbicules) can be related to their more evolved (biotite-bearing) counterparts by a process analogous to crystal fractionation. In contrast, the shells have nearly constant X_{Ca}, whereas the matrix has nearly constant Mg'. The orbicule cores apparently

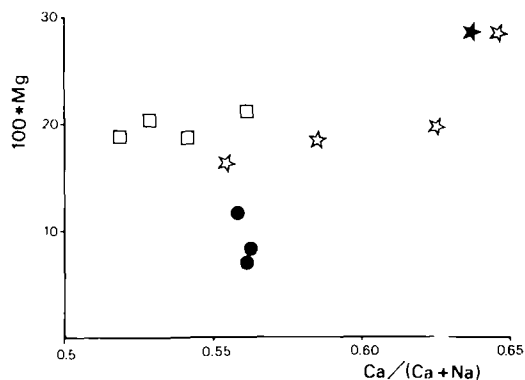FIG. 3. Mg' plotted against Ca/(Ca + Na). Symbols as in Fig. 2.

evolved toward a composition intermediate between the shell structures and the matrix (Fig. 3).

Together with the negative correlation (R = −0.86, all data) of CaO *versus* silica and the sympathetic variation of alkalis and silica concentrations (Fig. 2), this implies that the orbicule cores can be related compositionally to other parts of the diorite through the removal of component minerals.

To test this hypothesis, mass-balance calculations were undertaken to relate the major-element composition of a proto-orbicule with a primitive composition, to the orbicule core with the most evolved composition (Table 1). Mineral analyses used in the calculation correspond to the most calcic plagioclase (An_{51}), and the most magnesian biotite (X_{Mg} = 0.66) and hornblende (X_{Mg} = 0.56) in orbicule cores, and were taken from Owen (1991; Table 2, analyses 8, 7 and 6, respectively). The results indicate that the most evolved orbicule core can be derived from relatively primitive magma (represented by the proto-orbicule material) through the removal of 30% of the magma as plagioclase, hornblende and biotite in the proportions 91:6:3, respectively (Table 2). Despite the fact that three fractionating minerals were used in the calculation, the square of the weighted residuals of the calculation is high (R^2 = 2.85), principally because of a poor match for Si, Fe and Na.

The mass-balance data suggest that crystal fractionation was not the dominant control on the composition of the orbicule cores, a conclusion already anticipated by their high crystal/melt ratio, since it is unlikely that a crystal mush could allow effective fractional crystallization. The relatively small proportion of melt in the rock

Table 2

Petrogenetic modelling results for major elements

	Parent (proto-orb)	Daughter (evolved orb)	Daughter (model)
SiO$_2$	55.99	55.96	56.82
TiO$_2$	0.23	0.41	0.27
Al$_2$O$_3$	26.14	25.64	25.75
FeO$_t$	2.30	3.32	2.61
MnO	0.04	0.03	0.05
MgO	1.18	0.84	1.17
CaO	8.42	7.10	7.54
Na$_2$O	4.63	5.50	4.41
K$_2$O	1.09	1.10	1.39

Phases Removed	Proportions
Hbl	6.3
Pl	90.1
Bt	2.8

Magma remaining: 70%

R^2: 2.85

Notes: Major element oxides recalculated to 100 wt.% volatile-free. Major element concentrations of model estimated using mass balance calculations. Phase compositions are reported in Owen (1991) [see text].

therefore renders suspect variation diagrams using standard fractionation indicators (e.g. SiO$_2$, Mg') as tools to interpret magma evolution.

The enrichment of orbicule shells (relative to proto-orbicule material) in some of the same components as the 'evolved' cores is noteworthy, because the role of fractional crystallization has already been discounted. Although it might be argued that compositional contrasts between the cores and shells exclusively reflect variable crystal/melt ratios, the rhythmic layering of the shells, their uniformly fine grain size, and the xenomorphic nature of plagioclase preclude the likelihood that the feldspar in the shell structures is a cumulate phase. This suggests that the shells crystallized from what was essentially a crystal-free, supercooled melt that enveloped the crystal-melt core material. The orbicule cores nonetheless appear to have been chemically linked to the shells, possibly by the diffusion of primitive-melt components across the orbicule/matrix interface (see below), because both show similarly depleted levels of incompatible trace elements (Table 1).

It is likely that a process other than fractional crystallization or crystal accumulation controlled geochemical variations between the inner and outer parts of the orbicules. The small (centimetre-) scale of geochemical variations in the diorite, occurrence of the orbicules near the contact with the gneissic country rock of the diorite, and indirect evidence for supercooling in the orbicules suggests that Soret diffusion may

have been one such process. Although the importance of Soret diffusion in determining silica magma compositions has been challenged for many years (e.g. Bowen, 1921), the effects of thermodiffusion are likely to be detectable near the margins of volatile-rich magma chambers of high aspect ratio (Hildreth, 1981), provided that other mechanisms (e.g. fractional crystallization) were not prevalent. Several workers (e.g. Moore, 1984) have suggested that layered structures, including orbicules, may form as a result of changes in the relative rates of (1) mineral growth and (2) the diffusion of ions to sites of mineral growth. The present study proposes that in the case of the Run by Guess Island diorite, ionic diffusion was driven in part by small-scale thermal gradients across the boundary between water-rich crystal-melt globules and the surrounding magma, and led to the formation of the shell magma. Nucleation and diffusion processes responsible for the formation of the rhythmically-layered shell structures cannot, however, be evaluated from the available data.

As noted earlier, experimental data reported by Walker and DeLong (1982) demonstrate that geochemical changes induced in mafic silicate magma by Soret diffusion are the reverse of those resulting from crystal fractionation, but resemble those observed in immiscible silicate liquids. For example, the concentrations of relatively incompatible elements such as Si, Al, Na and K decrease down temperature gradients in silicate magma, whereas Fe, Mg, Ca and Cr increase. Because Fe is more sensitive to this process than Mg, then ferromagnesian phases should become more ferroan, while plagioclase becomes more calcic, down temperature gradients, provided that diffusion rates in the magma are suitably high.

Rigorous evaluation of Soret diffusion is hampered by the lack of bulk-rock data for individual light/dark shells, but the possible role of thermodiffusion within the orbicule structures, and between the orbicules and the matrix, can be ascertained from the available data. Although variations in plagioclase compositions across the shell structures are not reflected by corresponding variations in X_{Mg} values in biotite, which are nearly constant (Owen, 1991, Table 1), this does not necessarily negate bulk variations in Mg' between successive light or dark shells because other Fe-bearing phases (e.g. epidote, magnetite) are present, and biotite compositions could have been reset during subsequent, amphibolite-grade Grenvillian metamorphism in the area (cf. Owen et al., 1988). Moreover, limited data (3 analyses) for complete shell structures hint at a negative

correlation between Mg' and X_{Ca} (Fig. 3), as is expected for Soret diffusion.

The possible importance of Soret diffusion has been further evaluated by plotting the ratio of components (in this case alkalis/Ca) that can diffuse in opposite directions in silicate magma showing a pronounced temperature gradient, against fractionation indicators (Al, Mg'). The data are normalized to matrix values. Because Soret diffusion affects the concentrations of most major elements in the opposite sense to that of fractional crystallization, (Na + K)/Ca and differentiation indices such as Al and Mg' will systematically decline down a temperature gradient. Although representing a poor monitor of fractional crystallization because of the low proportion of melt, values of Mg' and Al can record Soret diffusion provided that the interstitial fluid permeated the crystal–melt mush.

Assuming that compositional differences between orbicules and the matrix result from ionic thermodiffusion, normalization of these component rations by matrix concentrations will yield coordinate values of less than unity if the orbicule magma was relatively cool, and greater than unity if the orbicules were relatively hot. Matrix-normalized plots of (Na + K)/Ca *versus* Al and Mg' for shells, cores, and bulk orbicule compositions (calculated by weighting shells and cores equally, consistent with their respective volumes) are shown in Fig. 4. Except for the proto-orbicule analysis, which plots as an outlier on both diagrams (Figs. 4A, B), the data show striking trends. (Na + K)/Ca in both shells and cores shows a strong negative correlation (excluding the proto-orbicule data, R = −0.92) with Al (Fig. 4A), but opposing behaviour ((Na + K)/Ca in shells increases; in cores, decreases) where plotted against Mg' (Fig. 4B). Because the Al content of plagioclase increases with anorthite content, the antithetic variation of (Na + K)/Ca with Al suggests that variations in the concentration of alumina are governed by the crystal/melt ratio rather than Soret diffusion.

The decline in matrix-normalized (Na + K)/Ca with increasing Mg' shown by orbicule cores contrasts with the sympathetic behaviour of these components in the shells (Fig. 4B). This suggests that the shell magma was derived from the interaction of the orbicule cores and relatively hot matrix magma, whereby Ca and alkalis diffused in opposite directions across the orbicule/matrix interface. The resulting contrasts in magma composition account for the presence of biotite (and absence of hornblende) in the shells.

The distribution of HFSE in the diorite is consistent with this interpretation. Although low
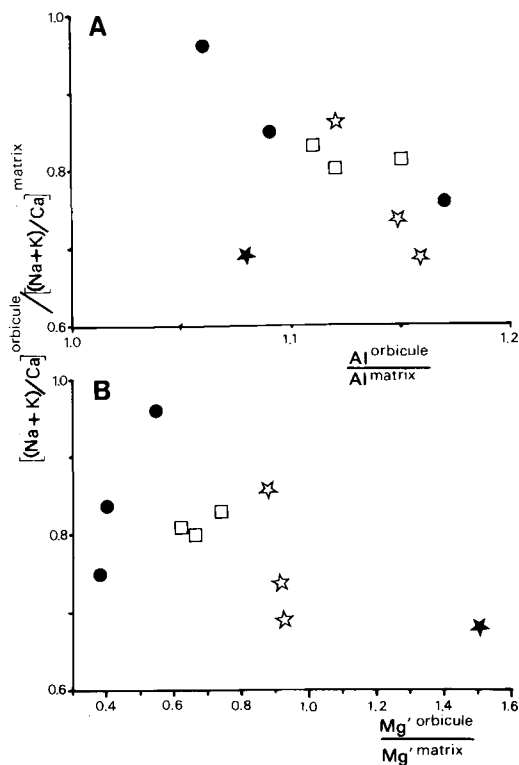

FIG. 4. Matrix-normalized plots showing the covariance of (Na + K)/Ca with Al (in A) and Mg' (in B) for orbicule shells (dots), cores (stars; closed star = proto-orbicule), and bulk orbicules (squares).

HFSE concentrations are indicative of high plagioclase/melt ratios in the orbicule cores, a different explanation is required to account for their similar depletion in the shells, which are interpreted to have been relatively melt-rich prior to consolidation. The inferred temperature gradient across the orbicule/matrix interface would promote diffusion not only of alkalis, but of other incompatible elements, including the HFSE, toward the relatively hot matrix magma. The relative concentrations of alkalis and HFSE in the shells and matrix suggest that the HFSE diffuse relatively rapidly along temperature gradients.

The composition of the proto-orbicule in sample 2 (Table 1) provides additional clues into the compositional evolution of the developing orbicule structures. Matrix-normalized (Na + K)/Ca and Mg' data for the bulk orbicules show a very restricted range of values of less than unity (Fig. 4B). In contrast, the proto-orbicule is depleted in (Na + K)/Ca compared with the bulk composition of well-developed orbicules, and has higher Mg' than the matrix. It therefore appears

that many of the orbicules became depleted in HFSE, and enriched in alkalis and Fe, as they developed shell structures. Unless variations in the rate of thermodiffusion of alkalis and Fe controlled small-scale compositional features of the orbicules, this implies (1) that other magmatic processes played a role in determining orbicule compositions, or (2) decoupling in the diffusional behaviour of alkalis and femic components, and suggests that diffusion mechanisms in mafic systems may not be entirely applicable to hydrated magmas of intermediate composition. The available data tend to support the latter hypothesis, but do not preclude the former.

The crystallization of the shells prior to the cores and matrix, and their fine grain size, is attributed to dewatering of the supercooled orbicules. The cores thereafter crystallized independently of the matrix, which fractionated toward a more evolved composition.

The Run By Guess Island orbicular diorite is by no means unique. Leveson (1963), for example, has reported calculated major-element compositions (based on mineral compositions and modes) for orbicular diorite from the Beartooth Mountains resembling the rocks described here. Like the Run By Guess Island occurrence, these orbicular rocks have elevated alumina (to 24 wt.% Al_2O_3) and lime (generally 5–7 wt.% CaO). The matrix is enriched in quartz, reflected by high bulk SiO_2, and depleted in Al, Fe, Mg and Na; the orbicules show an outward increase in Na/Ca, which Leveson (1963) attributed to the diffusion of Na and Ca in opposite directions during feldspar growth. By analogy with the rocks described herein, it appears that diffusion may have been promoted by a temperature gradient across the orbicule structures.

Unfortunately, too few geochemical data are reported in the literature to determine whether similar compositional patterns are characteristic of orbicular rocks in general. Available data do suggest, however, that the matrix material generally has a relatively evolved composition, a feature that must be taken into consideration by any model accounting for the origin of orbicules.

Conclusions

Orbicular diorite from Run by Guess Island has geochemical characteristics of a plagioclase-rich cumulate. The orbicule cores, in particular, had a high crystal/melt ratio, accounting for their extreme depletion in incompatible trade elements. The interstitial liquid in the orbicule cores was relatively water-rich, permitting supercooling and the establishment of a temperature gradient

across the orbicule/matrix interface. Thermodiffusional interaction between the orbicule fluids and the surrounding magma apparently led to the formation of the undercooled, relatively alkali- and Fe-rich shell magma. Although Soret diffusion may have played a role in determining some of the compositional contrasts (notably in alkalis, Ca and HFSE) between the orbicules and the matrix, it does not account for variations in Mg' values unless the thermodiffusional behaviour of these components differs in hydrated, intermediate magmas compared with mafic systems. The typical (but not universal) enrichment of the shell magma in alkalis suppressed the crystallization of hornblende. Dewatering of the orbicules quenched the shells, isolating the core material from further interaction with the matrix, which subsequently crystallized independently toward more evolved compositions.

References

Bowen, N. L. (1921) Diffusion in silicate melts. *J. Geol.*, **29**, 295–317.

Elliston, J. N. (1984) Orbicules: An indication of the crystallisation of hydrosilicates, 1. *Earth-Sci. Rev.*, **20**, 265–344.

Helz, R. T., Kirschenbaum, H. and Marinenko, J. W. (1989) Diapiric transfer of melt in Kilauea Iki lava lake, Hawaii: A quick, efficient process of igneous differentiation. *Geol. Soc. Amer. Bull.*, **101**, 578–94.

Hildreth, W. (1981) Gradients in silicic magma chambers: Implications for lithospheric magmatism. *J. Geophys. Res.*, **86**, 10153–92.

Leveson, D. J. (1963) Orbicular rocks of the Lonesome Mountain area, Beartooth Mountains, Montana and Wyoming. *Geol. Soc. Amer. Bull.*, **74**, 1015–40.

Moore, A. C. (1984) Orbicular rhythmic layering in the Palabora carbonatite, South Africa. *Geol. Mag.*, **121**, 53–60.

Owen, J. V. (1991) Significance of epidote in orbicular diorite from the Grenville Front zone, eastern Labrador. *Mineral. Mag.*, **55**, 173–81.

——Dallmeyer, R. D., Gower, C. F. and Rivers, T. (1988) Metamorphic conditions and $^{40}Ar/^{39}Ar$ geochronological contrasts across the Grenville Frong zone, coastal Labrador, Canada. *Lithos*, **21**, 13–35.

Philpotts, A. R. (1982) Compositions of immiscible liquids in volcanic rocks. *Contrib. Mineral. Petrol.*, **80**, 201–18.

Walker, D. and DeLong, S. E. (1982) Soret separation of mid-oceanic ridge basalt magma. Ibid., **79**, 231–40.